Completely inverted ClO vibrational distribution from OClO($^2A_2$ 24,0,0)

R. F. Delmdahl, B. L. G. Bakker, and D. H. Parker
Department of Molecular and Laser Physics, Catholic University of Nijmegen, NL-6525 ED Nijmegen, The Netherlands

(Received 22 November 1999; accepted 27 December 1999)

The gas phase dissociation dynamics of symmetric chlorine dioxide highly photoexcited into its $^2A_2$ 24,0,0 vibronic level has been investigated by monitoring both the kinetic energy release and the angular distribution of the O($^3P_2$) products via velocity map imaging. The resulting O($^3P_2$) kinetic energy profile provides full the vibrational distribution of the formed ClO($X\,^2\Pi, v$) radicals. The measured O fragment kinetic energy distribution reflects an unprecedented nonstatistical vibrational state population of their diatomic partners, where the excess energy is focused only in the three highest possible ClO vibrational levels $v=18-20$, with little fragment rotation. The anisotropy of the dissociation process sheds new light on the fragmentation dynamics of this stratospherically relevant triatomic molecule. © *2000 American Institute of Physics.* [S0021-9606(00)00112-4]

Due to its presumed influence on polar ozone,[1–3] there is a wealth of experimental and theoretical studies of the dynamical behavior of the OClO($^2A_2\nu_1,\nu_2,\nu_2$) fragmentation as well as on the wavelength dependent branching ratio of the dissociation channels involved, namely (ClO($X\,^2\Pi$) + O(^3P)) and (Cl(^2P) + O_2($^3\Sigma_g$,$^1\Delta_g$,$^1\Sigma_g$)). By now, it has been established that the OClO photodissociation in the gas phase leads almost exclusively to the formation of ClO radicals with only a few percent mode dependent contribution of the Cl atom channel at relatively low OClO photolysis energies (see Refs. 4–7, and references therein). The major dissociation channel in the gas phase, ClO+O, which is the subject in the present work, has been extensively studied over a great range of the OClO absorption spectrum, the distinct vibrational band structure of which reflects the quasibound character of the upper vibronic levels. The ClO and O fragments, respectively, were detected using schemes based on laser induced fluorescence (LIF) (Refs. 8 and 9) or resonant multiphoton ionization (REMPI),[10,11] whereas the O partners were monitored by REMPI time of flight[12] and photofragment translational energy spectroscopy.[13]

Peterson *et al.*[14] and very recently Guo *et al.*[15] calculated OClO potential energy surfaces proving that following initial dipole allowed excitation from the ground $^2B_1$ electronic state into the $^2A_2$ state the fragmentation process is influenced by two neighboring potential surfaces, i.e., the $^2A_1$ and the $^2B_2$ surface. From the *ab initio* potentials for the optically excited $^2A_2$ state and the close-lying $^2A_1$ state, a barrier to dissociation of ≈0.4 eV along the asymmetric coordinate is found. This is in a rather good agreement with earlier linewidth measurements, where a substantial broadening of the rotational lines in this energy region due to the necessary coupling into the $^2B_2$ state has been observed.[16] At higher photolysis energies (>3.1 eV) where basically all three potential surfaces are open to an asymmetrical decay, there is still some speculation about the dynamical behavior of the fragmentation proceeding either directly via the $^2A_2$ or indirectly via the $^2A_1$ and $^2B_2$ surface, respectively.

In the present work, photodissociation of jet-cooled OClO in the short wavelength region of its first electronic absorption band ($X\,^2B_1 \rightarrow {}^2A_2$) (Ref. 17) is examined using the recently developed velocity map imaging technique. We show that the recoil of the ClO and O fragments is highly anisotropic, and that the available energy of the process is channeled almost entirely into ClO vibration. On the basis of theoretical results, and from a mechanistic viewpoint,[18] this indicates a virtually linear geometry of the decaying parent evolving along the $^2A_1$ potential energy surface.

The employed experimental apparatus and as well the technique of velocity mapping, an advanced variant of ion imaging,[19] have been reported in detail previously[20,21] and will be summarized only briefly in this Communication. A pulsed supersonic expansion of 3%–5% OClO seeded in He at atmospheric pressure is directed along the axis of a time of flight spectrometer and after passing a skimmer of 1 mm diam encounters two counter propagating pulsed dye laser beams at right angles. The background pressure in the time of flight region of the vacuum chamber during the measurements of about 3×10^{-7} Torr is achieved using an oil diffusion pump for the main chamber and a turbomolecular pump further evacuating the time of flight tube. The required photolysis wavelength of 281 nm is generated using a Nd:YAG-pumped dye laser (Spectra-Physics DCR-2A; PDL-2) with dye Rhodamine 6G followed by frequency doubling the output in a KDP crystal. A second Nd:YAG-pumped dye laser system (Spectra-Physics GCR-11; PDL-2) with dye Coumarin 47 and frequency doubling in a BBO crystal delivers the detection laser light around 226 nm. Both laser systems operate at 10 Hz and the laser pulses are focused on the molecular beam pulse by 200 mm quartz lenses. The detection laser pulse (pulse duration ~5 ns, output energy after doubling ~0.5 mJ) arrives with a temporal delay of 20–30 ns after the photolysis laser pulse (pulse duration ~5 ns output energy after doubling 1–3 mJ). The recoiling O(^3P) photofragments are monitored via resonant two-photon excitation of the well-known ($2p\,^3P_2 \rightarrow 3p\,^3P_2$)-transition with

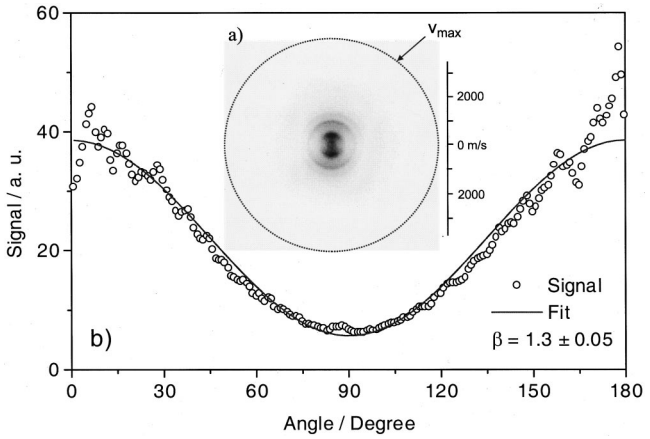

FIG. 1. (a) Raw ion image of $O(^3P_2)$ originating from $OClO(^2A_2\ 24,0,0)$. The polarization direction of both the dissociation and the detection laser are along the vertical axis of the image. Signal strength increases from white (background) to black (highest intensity). The calibration bar shows the relation of ion position and speed. (b) Angular distribution obtained for the $ClO(v=19)$ vibrational band (open dots). A fit (solid line) to the obtained data yields a rather high anisotropy parameter $\beta=1.3\pm0.05$.

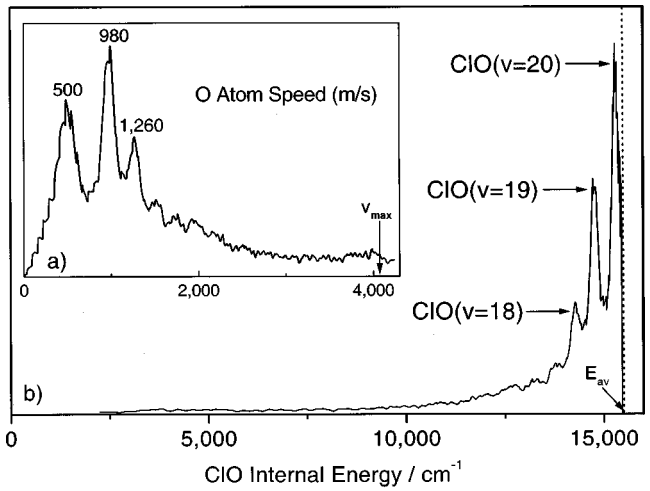

FIG. 2. (a) Speed distribution of $O(^3P_2)$ fragments obtained from the measured data represented in (a) indicating the low kinetic energy release. (b) ClO internal energy distribution calculated from the speed distribution of the O partner atoms depicted in (a). Essentially only the highest possible ClO vibrational levels $v=18-20$ (marked by arrows) are populated.

subsequent ionization $(2+1)$REMPI using a wavelength of 225.6 nm. In order to provide equal sensitivity for each fragment velocity, the detection laser wavelength is scanned repetitively across the entire Doppler profile of the $O(^3P_2)$REMPI transition. The ion signal vanishes completely when the photolysis laser is blocked or when the two foci do not overlap. An electrostatic immersion lens accelerates ions of equal velocity to the same point of a position sensitive ion-detector which consists of an array of two microchannel plates (MCP), a phosphor screen, and a CCD camera (LaVision, 384×286 pixles). Mass selectivity is achieved by gating the front MCP. Averaging over 5000 laser shots is sufficient to produce the raw 2D image, from which the inherent three-dimensional fragment distribution is reconstructible using a Hankel inversion algorithm.

OClO is synthesized according to the method described by Derby and Hutchinson[22] by flowing a 3% mixture of Cl_2 diluted in He at atmospheric pressure through a U-tube containing sodium chlorite and glass beads. The yellow–green reaction product is carried via teflon tubing directly to the expansion nozzle.

In order to examine the beam conditions, vibrational bands of $OClO(^2A_2)$ were recorded in the investigated region with the photofragment yield method,[23] detecting the total $O(^3P_2)$ atom yield while tuning the photolysis laser. From a comparison of the overall appearance of these OClO bands, which show rotational structure, with calculated transitions[16] the rotational temperature of the parent molecule in the beam is estimated to be below $T_{rot}\sim50$ K. The full angular as well as kinetic energy distribution of O products observed after preparing OClC in its predissociative $^2A_2$24,0,0 vibronic level is depicted in the raw 2D image in Fig. 1(a). Darker regions correspond to the higher O^+ ion signal intensity. The polarization vectors of the dissociation and the detection lasers are parallel to the image plane and lie along the vertical axis of the figure. It is obvious from the two rings which are clearly discernible in the ion image that the atomic fragments are located to a great extent relatively close to the middle of the detector, i.e., at very low kinetic energies, exhibiting a $\sim\cos^2$ distribution of the velocity vectors. The strongest innermost ring corresponds to O partners recoiling at a velocity of ~500 m/s in the fragmentation process and hence, carrying negligible amounts of kinetic energy. The next following ring which also appears very intense in the image has a radius corresponding to an atomic fragment velocity of ~980 m/s correlating with a mere ~5% of the available energy ending up as product translation.

The open circles shown in Fig. 1(b) depict the measured angular distribution of $O(^3P_2)$ products corresponding to $ClO(v=19)$ which exhibits a significant anisotropy of the recoiled fragments. The maximum signal is visible at 0° and 180° relative to the vertical polarization axis of the laser beams. Fitting the experimental data by using the equation $I(\theta)=1+\beta P_2(\cos\theta)$, where $P_2(\cos\theta)$ represents the second order Legendre Polynomial, a value of $\beta=1.3\pm0.05$ is obtained. The values of the anisotropy parameters determined for the other ClO vibrational levels ($v=18$ and $v=20$) are found to be the same within the limit of error.

Due to energy and momentum conservation, the O kinetic energy distribution extracted from the corresponding speed distribution shown in Fig. 2(a), directly mirrors the ClO partner internal energy distribution which is represented in Fig. 2(b). It is seen in Fig. 2(b) that almost the total energy available for the fragments is converted into product vibrational energy; only ClO vibrational levels starting from $v=18$ and increasing up to $v=20$ are populated. The energetic threshold of the process, given by $E_{av}=E_{nv}-D_0$, where E_{nv} is the photon energy and D_0 is the dissociation energy of OClO,[4] is indicated by the dotted vertical line in Fig. 2(b). Contrary to earlier experiments at longer photodissociation wavelengths based on photofragment translational energy methods,[5,12,13] the employed velocity mapping technique allows for the complete ClO vibrational state analysis. Since the observed vibrational bands of ClO are clearly sepa-

rated, a moderate fragment rotational excitation in the order of 200 K is assumed. Furthermore, a rather low contribution of spin–orbit excited $ClO(X\,^2\Pi_{1/2})$, which should otherwise be clearly visible,[8] can be expected.

Based on the calculations of Peterson and Werner,[14] the measured value of the anisotropy parameter $\beta = 1.3 \pm 0.05$ can only be rationalized with an indirect predissociation pathway along the $^2A_1$ surface. This surface is accessible via spin–orbit coupling, and exhibits an equilibrium bond angle of 120° with only a shallow barrier to linearity, which is particularly suited to lead to the observed high anisotropy parameter. From our measured anisotropy parameter and based on a near linear decay geometry, we calculate a relatively long lifetime of $OClO(^2A_2\,24,0,0)$ of ~700 fs which also points to an indirect mechanism. Following the initial optical preparation of highly excited $OClO(^2A_2\,24,0,0)$, and spin–orbit coupling into the $^2A_1$ surface, the parent molecule has to accumulate ≈0.4 eV of asymmetric stretch excitation in order to pass the barrier to product formation. This barrier exists for decay along the asymmetric coordinate of the quasilinear $^2A_1$ state. Consequently, the observed high recoil anisotropy as well as the vibrational energy focussing can readily be induced in the exit channel.

This picture of a quasilinear decay of the triatomic parent along the $^2A_1$ surface is assisted by very recently reported theoretical results of Guo and co-workers.[15] In their work they observed that a bifurcation arises for the $^2A_2\,5,0,0$ level which is predicted to grow with increasing $(\nu_1,0,0)$-excitation of $OClO(^2A_2)$, promoting an asymmetric motion of the initially $(^2A_2\,24,0,0)$-excited OClO. An adiabatic predissociation directly along the optically prepared $^2A_2$ state with an equilibrium bond angle of ~107° can be excluded, since the anisotropy parameter is then restricted to a maximum value of $\beta_{max} = 0.93$ according to simple impulsive model considerations.[18] For the same aspect, the possible decay of $OClO(^2A_2\,24,0,0)$ along the strongly bent $^2B_2$ state, which is attainable from the $^2A_1$ surface by asymmetric stretch coupling, should also be precluded.

In conclusion, mapping the velocities of $O(^3P_2)$ atoms formed in the photofragmentation of $OClO(^2A_2\,24,0,0)$ a nearly complete conversion (~95%) of the huge energy available in the process into ClO vibrational states $v = 18-20$ has been found. The obtained angular distribution is well rationalized with a quasilinear O–ClO decay along the $^2A_1$ potential energy surface. The observation of nearly exclusive $ClO(v = 18-20)$ production from OClO is particularly striking regarding the important role these trace gas constituents play in Earth's stratospheric chemistry.[1,24] In particular, vibrationally excited ClO has already been found to be much more reactive than ground state ClO.[25] In addition, a considerable red shift of the ClO absorption band[26] should be observed which facilitates their dissociation, leading to a new mechanism for direct release of Cl atoms in the stratosphere.

This work is supported by the European Union TMR program IMAGINE. Contract No. ERB 4061 PL 97-0264, and by the ''Stichting voor Fundamenteel Onderzoek der Materie'' (FOM), which is financially supported by the ''Nederlandse Organisatie voor Wetenschappelijk Onderzoek'' (NWO). Technical assistance by Cor Sikkens and Chris Timmer is gratefully acknowledged.

[1] S. Solomon, Nature (London) **347**, 347 (1990).
[2] V. Vaida and J. D. Simon, Science **286**, 1443 (1995).
[3] V. Vaida, S. Solomon, E. C. Richard, E. Rühl, and A. Jefferson, Nature (London) **342**, 405 (1989).
[4] H. F. Davis and Y. T. Lee, J. Chem. Phys. **105**, 8142 (1996).
[5] H. F. Davis and Y. T. Lee, J. Phys. Chem. **100**, 30 (1996).
[6] R. F. Delmdahl, S. Ullrich, and K.-H. Gericke, J. Phys. Chem. A **102**, 7680 (1998).
[7] T. Baumert, J. L. Herek, and A. H. Zewail, J. Chem. Phys. **99**, 4430 (1993).
[8] S. Baumgärtel and K.-H. Gericke, Chem. Phys. Lett. **227**, 461 (1994).
[9] Y. Matsumi and S. M. Shamsuddin, J. Chem. Phys. **103**, 4490 (1995).
[10] E. Rühl, A. Jefferson, and V. Vaida, J. Phys. Chem. **94**, 2990 (1990).
[11] C. J. Kreher, R. T. Carter, and J. R. Huber, Chem. Phys. Lett. **286**, 389 (1998).
[12] M. Roth, C. Maul, and K.-H. Gericke, J. Chem. Phys. **107**, 10582 (1997).
[13] A. Furlan, H. A. Scheld, and J. R. Huber, J. Chem. Phys. **106**, 6538 (1997).
[14] K. A. Peterson and H.-J. Werner, J. Chem. Phys. **96**, 8948 (1992).
[15] D. Xie and H. Guo, Chem. Phys. Lett. **307**, 109 (1999).
[16] E. C. Richard and V. Vaida, J. Chem. Phys. **94**, 163 (1991).
[17] A. Wahner, G. S. Tyndall, and A. R. Ravishankara, J. Phys. Chem. **91**, 2734 (1987).
[18] R. Schinke, *Photodissociation Dynamics* (Cambridge University Press, Cambridge, 1993).
[19] D. W. Chandler and P. L. Houston, J. Chem. Phys. **87**, 1445 (1987).
[20] A. T. J. B. Eppink and D. H. Parker, Rev. Sci. Instrum. **68**, 3477 (1997).
[21] D. H. Parker and A. T. J. B. Eppink, J. Chem. Phys. **107**, 2357 (1997).
[22] R. I. Derby and W. S. Hutchinson, Inorg. Synth. **4**, 152 (1953).
[23] H. Reisler and C. Wittig, Annu. Rev. Phys. Chem. **37**, 307 (1986).
[24] J. Sessler, M. P. Chipperfield, J. A. Pyle, and R. Toumi, Geophys. Res. Lett. **22**, 687 (1995).
[25] R. F. Delmdahl and K.-H. Gericke, Chem. Phys. Lett. **281**, 407 (1997).
[26] M. Mandelman and R. W. Nicholls, J. Quant. Spectrosc. Radiat. Transf. **17**, 483 (1977).